



HAL
open science

Novel configuration of a three-phase induction generator for single-phase load: simulations and experimentations

Bunthern Kim, Maria Pietrzak-David, Pascal Maussion

► To cite this version:

Bunthern Kim, Maria Pietrzak-David, Pascal Maussion. Novel configuration of a three-phase induction generator for single-phase load: simulations and experimentations. IECON 2019, Oct 2019, Lisbon, Portugal. pp.5807-5813. hal-03113732

HAL Id: hal-03113732

<https://hal.science/hal-03113732>

Submitted on 18 Jan 2021

HAL is a multi-disciplinary open access archive for the deposit and dissemination of scientific research documents, whether they are published or not. The documents may come from teaching and research institutions in France or abroad, or from public or private research centers.

L'archive ouverte pluridisciplinaire **HAL**, est destinée au dépôt et à la diffusion de documents scientifiques de niveau recherche, publiés ou non, émanant des établissements d'enseignement et de recherche français ou étrangers, des laboratoires publics ou privés.



Open Archive Toulouse Archive Ouverte

OATAO is an open access repository that collects the work of Toulouse researchers and makes it freely available over the web where possible

This is an author's version published in: <https://oatao.univ-toulouse.fr/27212>

Official URL:

<https://doi.org/10.1109/IECON.2019.8927218>

To cite this version:

Kim, Bunthern^{ORCID} and Pietrzak-David, Maria^{ORCID} and Maussion, Pascal^{ORCID} *Novel configuration of a three-phase induction generator for single-phase load: simulations and experimentations.* (2019) In: IECON 2019, 14 October 2019 - 17 October 2019 (Lisbon, Portugal).

Any correspondence concerning this service should be sent to the repository administrator: tech-oatao@listes-diff.inp-toulouse.fr

Novel Configuration of a Three-phase Induction Generator for Single-phase Load: Simulations and Experimentations

Bunthern Kim, Maria Pietrzak-David, Pascal Maussion
LAPLACE, Université de Toulouse, INP, UPS, CNRS, Toulouse,
France

Email : pascal.maussion@laplace.univ-tlse.fr

Abstract— This paper presents the study of an original configuration of an off-grid single-phase generator using a three-phase Squirrel Cage Induction Machine (SCIM). In this proposed structure, two of the generator stator windings are excited by two independent sources and the remaining winding is connected to the load. This configuration requires two voltage inverters for excitation. This allows better control flexibility in the inverter-assisted topology. Simulation model of the generator has been created to study its dynamic and steady-state characteristics. These behaviors of the generator have been verified using comprehensive laboratory tests. The use of this generator configuration is proposed according to the concept of frugal innovation to propose cheap solutions for rural electrification in remote areas in developing countries.

Keywords—Induction generator; inverter-assisted; simulation and experimentation; frugal innovation;

NOMENCLATURE

$[V_s]$: Stator voltages in 'abc' frame, $[v_{sa}, v_{sb}, v_{sc}]^T$
$[I_s]$: Stator currents in 'abc' frame, $[i_{sa}, i_{sb}, i_{sc}]^T$
$[V_r]$: Rotor voltages in 'abc' frame, $[v_{ra}, v_{rb}, v_{rc}]^T$
$[I_r]$: Rotor currents in 'abc' frame, $[i_{ra}, i_{rb}, i_{rc}]^T$
$[V_{s_dq0}]$: Stator voltages in 'dq0' frame, $[v_{sd}, v_{sq}, v_{s0}]^T$
$[I_{s_dq0}]$: Stator currents in 'dq0' frame, $[i_{sd}, i_{sq}, i_{s0}]^T$
$[I_{r_dq0}]$: Rotor currents in 'dq0' frame, $[i_{rd}, i_{rq}, i_{r0}]^T$
R_s, R_r	: Stator/rotor phase resistance
L_s, L_r	: Stator and rotor cyclic inductance
M	: Mutual cyclic inductance
θ, ω	: Rotor electrical angular position/ rotation speed
θ_s, θ_r	: Electrical angular position between magnetic field and stator/rotor
V_{e1}, V_{e2}	: Excitation voltage sources
I_{e1}, I_{e2}	: Excitation currents
C, R_L	: Excitation capacitor, load resistance
i_C, i_L	: Capacitor current, load current
P	: Number of poles.
T_p	: Torque given by turbine.
T_e	: Electromagnetic torque.

I. INTRODUCTION

Providing electricity access to rural villages in developing countries through power grid extension faces many challenges including investment costs, low profitability and requires long term planning. A small-scale distributed generation system developed for supplying local households may provide

immediate solution. However, cost and sustainability will not be improved if it depends on diesel or coal based generator systems. Renewable resources such as solar, hydro and wind could provide free and sustainable energy. To minimize the cost, we proposed the concept of reusing electrical and electronics equipment and batteries in a small standalone renewable energy system. This concept is illustrated in Fig. 1.

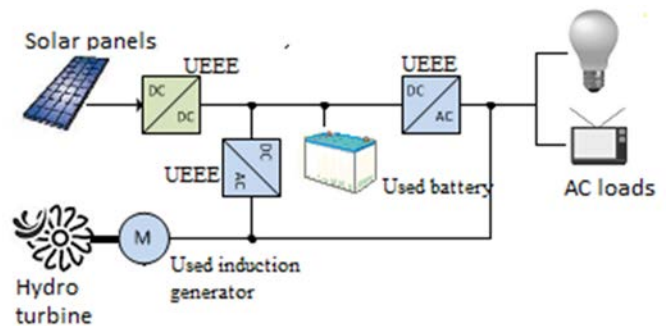


Fig. 1. Proposed renewable energy system based on reuse of Used Electronics and Electrical Equipment (UEEE).

In renewable energy systems, induction generators are often employed due to their advantageous features over synchronous generators, such as robustness, low cost, brushless construction, and low maintenance cost. Moreover, due to its ubiquity, induction motors are the perfect choice for a 2^o life use in pico-hydro or wind energy system. Most autonomous power systems and loads are based on single-phase distribution schemes and the use of single-phase induction machine is limited to relatively small power outputs. At power ratings above 3kW, three-phase induction generators are preferred over single-phase generators due to their advantages of lower weight, lower cost, and higher availability [1, 2].

The operation of three-phase self-excited induction machines as stand-alone, single-phase generator with fixed excitation source has been widely studied. The three-phase machine operated as a single-phase generator works under a very unbalanced condition. There are several balancing methods which are based on passive circuit elements (excitation capacitors, impedances) and on power electronic converters. Four distinctive balancing configurations based on capacitors are proposed in [3]. For voltage regulation, an Electronic Load Controller (ELC) that dissipates the exceeding active power can also be used with the capacitor excitation configuration [4].

However, these self-excited techniques suffer from unsatisfactory voltage regulation and frequency variations.

Improved voltage regulation while operating at balanced condition can be obtained by a combination of a three phase voltage source inverter (VSI) or static compensator (STATCOM) and an ELC, operating with parallel excitation capacitor [5, 6]. The disadvantage is that the frequency will change with the rotation speed since there is no frequency decoupling between load and generator. The optimal performance under varying speed and load conditions can be obtained by using two power converters in back-to-back configuration (or AC-DC-AC link) [7]. Nevertheless, this straightforward solution has the highest cost and complexity.

An original configuration of a single-phase generator based on 3-phase induction squirrel cage machine without back-to-back converter stage has been recently proposed in [8, 9]. This technique uses a two-series-connected-and-one-isolated (TSCAOI) phase winding configuration where one of the three windings is for excitation. The two remaining windings are connected in series and serve as the winding for the single-phase electricity generation at the output. A battery storage system and a power converter are required to supply the excitation winding. This topology can provide output voltage regulation while keeping the frequency constant at a variable rotation speed. The battery storage also helps to compensate the fluctuation of energy demand by storing the energy when the consumption is low and supplying energy when the consumption is high or the available renewable energy is low.

A new inverter-assisted topology based on the TSCAOI configuration has been proposed and presented in [10] as shown in Fig. 2. This technique uses a One-Isolated-And-Two-Isolated-Inputs or OIATI winding configuration where two of the stator windings are excited by two separated sources. The third winding, with a parallel capacitor, provides the output power to the connected loads. The excitation sources may be provided by two bidirectional inverters powered by a battery storage system. Although this topology introduces extra complexity and cost by requiring a second excitation inverter, it could allow a reduced current rating requirement for the inverters, as well as improve the dynamic performance of the generator and increase the number of degrees of freedom available for control purposes.

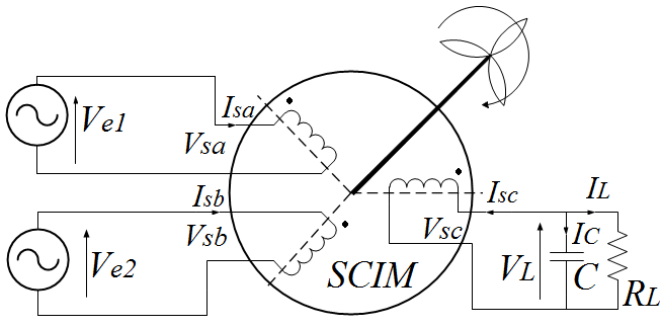


Fig. 2. Proposed single-phase induction generator based one three-phase SCIM.

This paper presents further results of both simulations and experimentations of the proposed generator configuration

working in open loop. Two AC voltage sources with the same frequency are employed to supply the excitation windings.

II. DYNAMIC MODELING

A. DQ state-space model of the induction generator

As presented in [10], if stator and rotor currents are chosen as state variables and the output is connected to a resistive load (without capacitor) the state equation in ‘ $dq0$ ’ reference frame can be expressed as follows:

$$\frac{d}{dt} [x] = \begin{bmatrix} [A'_{11}] & [A'_{12}] \\ [A'_{21}] & [A'_{22}] \end{bmatrix} [x] + \begin{bmatrix} [B_{11}] \\ [B_{21}] \end{bmatrix} [u'] \quad (1)$$

$$\text{Where: } [A'_{11}] = \begin{bmatrix} -\frac{R_s L_r}{\beta} & \frac{\omega_s L_s L_r - \omega_r M^2}{\beta} & 0 \\ \frac{-\omega_s L_s L_r + \omega_r M^2}{\beta} & -\frac{R_s L_r}{\beta} & 0 \\ 0 & 0 & -\frac{(R_s + R_L)}{L_{s0}} \end{bmatrix};$$

$$[A'_{12}] = \begin{bmatrix} \frac{R_r M}{\beta} & \frac{L_r M}{\beta} (\omega_s - \omega_r) \\ \frac{L_r M}{\beta} (\omega_r - \omega_s) & \frac{R_r M}{\beta} \\ 0 & 0 \end{bmatrix};$$

$$[A'_{21}] = \begin{bmatrix} \frac{R_s M}{\beta} & \frac{L_s M}{\beta} (\omega_r - \omega_s) & 0 \\ \frac{L_s M}{\beta} (\omega_s - \omega_r) & \frac{R_s M}{\beta} & 0 \end{bmatrix};$$

$$[A'_{22}] = \begin{bmatrix} -\frac{R_r L_s}{\beta} & \frac{\omega_r L_s L_r - \omega_s M^2}{\beta} \\ \frac{-\omega_r L_s L_r + \omega_s M^2}{\beta} & -\frac{R_r L_s}{\beta} \end{bmatrix};$$

$$[B_{11}] = \begin{bmatrix} \frac{L_r}{\beta} & 0 & 0 \\ 0 & \frac{L_r}{\beta} & 0 \\ 0 & 0 & \frac{1}{L_{s0}} \end{bmatrix}; [B_{21}] = \begin{bmatrix} -\frac{M}{\beta} & 0 & 0 \\ 0 & -\frac{M}{\beta} & 0 \\ 0 & 0 & 0 \end{bmatrix}; \beta = L_s L_r - M^2$$

The state and input vectors are defined by:

$$[x] = [i_{sd}, i_{sq}, i_{s0}, i_{rd}, i_{rq}]^T;$$

$$[u'] = [V_{e_dq0}] = [P(\theta_s)] [V_e] = [v_{ed}, v_{eq}, v_{e0}]^T; \text{ where:}$$

$$[V_e] = \begin{bmatrix} v_{sa} \\ v_{sb} \\ 0 \end{bmatrix} = \begin{bmatrix} v_{e1} \\ v_{e2} \\ 0 \end{bmatrix}; [P(\theta_s)] \text{ is the 'Park' transformation matrix.}$$

M_{sr} is the maximal mutual inductance between ‘‘a’’ stator phase and ‘‘a’’ rotor phase. ‘ θ ’ is the electrical angle between ‘‘a’’ rotor and ‘‘a’’ stator phase. The position of the rotating magnetic field is defined by the angle θ_s in relation to stator reference frame and by the angle θ_r in relation to rotor reference one. Consequently, the relation between these three angles and the corresponding stator, rotor and electrical velocities can be written in (2) and (3):

$$\theta_s = \theta + \theta_r \quad (2)$$

$$\omega_s = \frac{d\theta_s}{dt}; \omega_r = \frac{d\theta_r}{dt}; \omega = \frac{d\theta}{dt} \quad (3)$$

L_s and L_r are stator and rotor cyclic inductances; L_{s0} and L_{r0} inductances correspond to homopolar components of stator and rotor voltages and M is the mutual cyclic inductance ($M = \frac{3}{2}M_{sr}$). The model usually assumes that the magneto-motive forces created by the stator and rotor phases are spread in a sinusoidal way along the air gap and without saturation.

When the capacitor is included, an additional differential equation can be derived at the output winding as the following:

$$\begin{cases} v_{sc} = R_L i_L \\ C \frac{d}{dt} v_{sc} = i_C = -i_{sc} - i_L \end{cases} \quad (4)$$

$$\Leftrightarrow \frac{d}{dt} i_L = -\frac{1}{R_L C} i_L - \frac{1}{R_L C} i_{sc} \quad (5)$$

$$i_{sc} = \sqrt{\frac{2}{3}} \begin{bmatrix} \cos(\theta_s - \frac{4}{3}\pi) & -\sin(\theta_s - \frac{4}{3}\pi) & \frac{1}{\sqrt{2}} \end{bmatrix} [i_{sd}, i_{sq}, i_{s0}]^T \quad (6)$$

Following the derived equation in (5), i_L can be incorporated into a state variable using the relationship of equation (6), in which the stator current is converted to $dq0$ reference frame. As a result, the new state space equation involves terms which are dependent to rotor and magnetic field position. Although it is possible to remove the non-constant parameter by adding new variables and transforming equation (5) into $dq0$ frame, the new model will face the problem where both inputs and output are not independent [10]. The dynamic of the SCIM shaft can be obtained from mechanical equation which is derived as:

$$\frac{d\omega}{dt} = \frac{P}{2J} (T_p - T_e) - \frac{D}{J} \omega \quad (7)$$

T_p is torque given by turbine. The electromagnetic torque T_e developed in induction generator using stator and rotor currents is expressed in (8), where P is the number of poles of the generator; J is the overall system inertia and D viscous friction coefficient:

$$T_e = \frac{P}{2} M (i_{sq} i_{rd} - i_{sd} i_{rq}) \quad (8)$$

B. Transient response

The equations developed above have been implemented in Matlab/Simulink®, to simulate the system behavior and to obtain its response for a given situation. Experimentations are conducted with using a 1.5kW, 4 poles induction generator whose shaft is connected to another induction motor as depicted in Fig. 3. The generator equivalent circuit parameters (referred to the stator) are given in Table I. The generator is excited by fixed sinusoidal sources ($Ve1=Ve2$) with a phase difference of 120° . Since the AC sources cannot absorb all the active power given by the generator, compensation loads are employed in parallel to the generator windings. The additional resistive loads keep the active power from flowing back into the AC sources power supply. The generator is rotated in the same direction that it would run if it was only driven by the voltage sources alone (without motor drive). The output of the generator is connected

to a $30\mu\text{F}$ capacitor and 30Ω loads. The capacitor helps minimizing the winding currents and increasing the output voltage. To illustrate its dynamic behavior, the generator is driven at a constant speed of 1540rpm. Simulated and test results of the transient response of input currents and output voltage are illustrated in Fig. 4 and Fig. 5.

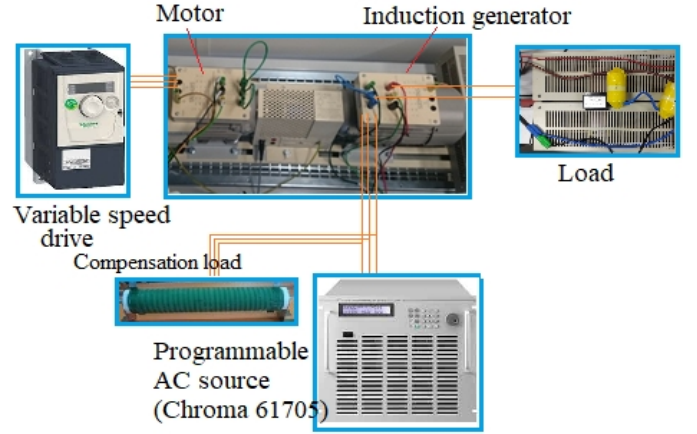


Fig. 3. Experimental setup.

TABLE I. A 1.5kW GENERATOR PARAMETERS

	Value
Rated voltage	220/380 V
Stator/rotor resistance	3.84/3.94 Ω
Stator/rotor leakage inductance (l_{sb}, l_{rl})	0.025 H
Magnetization inductance (M_{sr})	0.388 H
Number pole	4
Moment of inertia	0.01 Kg.m ²

High initial currents can be observed in the excitation phases. They quickly reach steady state after a few periods. To avoid this issue, the input voltage should be increased gradually to the desired value. Meanwhile, the outputs reach steady-state without overshoot.

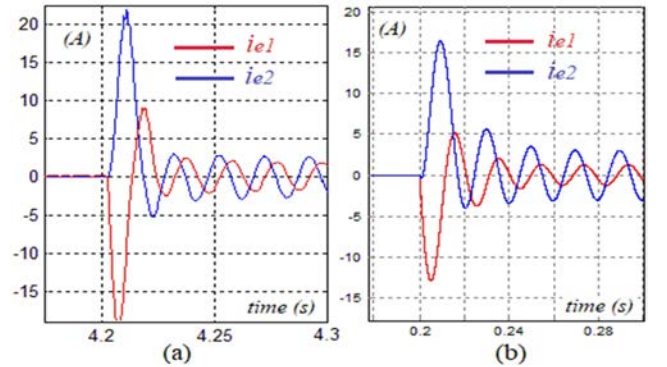


Fig. 4. Transient response of input winding currents ($Ie1, Ie2$): (a) test results; (b) simulated results.

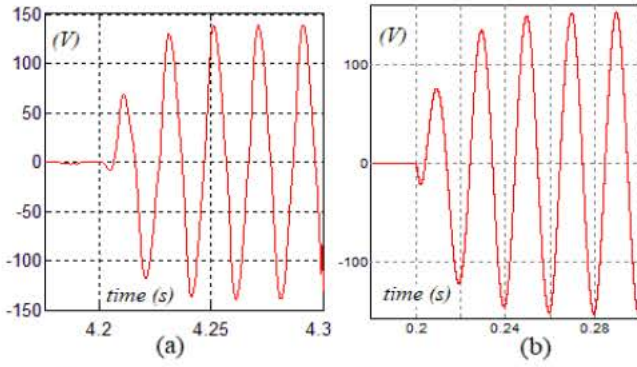


Fig. 5. Transient response of the output voltage (V_{sc}): (a) test result; (b) simulated result.

III. STEADY-STATE STUDY

A. Simulation study

To further evaluate the performance of the proposed OAITI generator configuration, simulation models are implemented in PSIM. The system can be either driven by a constant-speed or a constant-power prime mover connected to its shaft. It should be noted that if the moment of inertia is high enough, the generator will be rotated at nearly constant speed when driven by constant-power prime mover. The excitation sources $Ve1$ and $Ve2$ are simulated using ideal sinusoidal voltage sources at 50Hz. The rated output voltage is 220Vrms at the same frequency.

a) Sizing of output capacitor

To explain the choice of output's capacitor in this simulation, the generator is driven by a constant mechanical power and the excitation voltage ($Ve1/Ve2$) is kept at 212Vrms. $Ve1$ phase leads $Ve2$ phase by 120° . The steady-state values of the generator for different capacitor values are depicted in Fig. 6, Fig. 7 and Fig. 8. The influence of the capacitor value on the output voltage of the generator can be seen clearly in Fig. 6. It also has the effect on the winding current due to increased reactive power. Increased capacitor size provides more reactive power to generator and reduces the reactive powers provided by the input windings. This results in increased current in the output winding and reduced currents in the input windings, as shown in Fig. 7 and Fig. 8. The optimization of all winding currents can be obtained by choosing capacitor value between $20\mu\text{F}$ and $30\mu\text{F}$. This optimization might depend on the limitation of each winding which is not necessarily the same.

b) Feasible operation range

In this study, the generator is rotated at a speed which varies between 1460rpm to 1660rpm. The output voltage is kept at 220Vrms by adjusting the excitation voltage sources. $Ve1$ phase always leads $Ve2$ phase by 120° . The excitation capacitor for the output phase is $30\mu\text{F}$. The steady-state simulation results for light load (50W) and normal load (500W) are shown in Fig. 9, Fig. 10 and Fig. 11. Fig.9 show that the reactive powers absorbed by the generator are always positive and are minimal at just above the synchronous speed (1500rpm). As shown in Fig. 10,

the winding currents change in similar way as the reactive power.

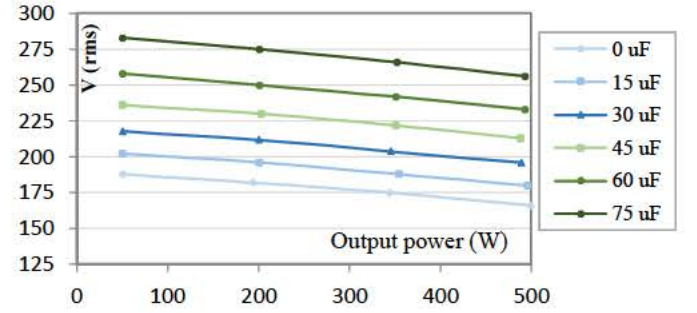


Fig. 6. Output voltage for various capacitor values as a function vs output power.

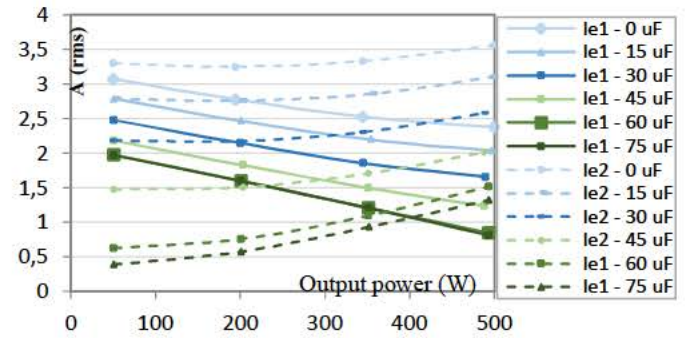


Fig. 7. Excitation winding currents for various capacitor values vs output power.

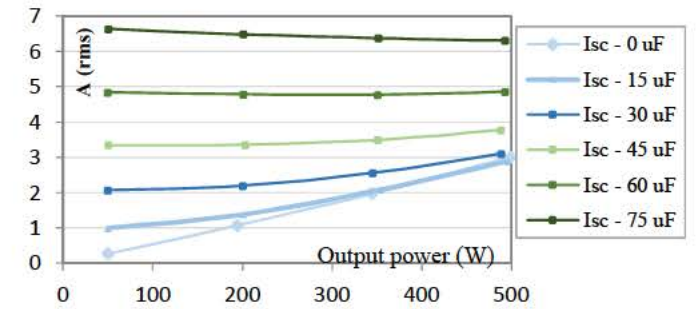


Fig. 8. Output winding current for various capacitor values vs output power.

The active powers provided by the excitation sources are positive at low speed and negative above a certain speed. This speed is slightly different for the two excitation windings and also depends on the load. Induction machine only generates active power above synchronous speed. Below this speed, the generator will become a burden by acting as an induction motor. In this case, power is transferred from the excitation sources to both the generator and the output. Above 1500rpm, the generator also becomes the source of active power. However the active power from excitation sources is still required. Based on Fig. 9, all the active powers from excitation sources become negative at speed above 1520rpm. In this case, all the active power is provided by the generator.

The feasible operation region can be limited to rotation speeds above 1500rpm. The upper bound of the region is limited by the rating of winding currents, core saturation and rated torque of the generator. The generator also functions at lower speed than 1500rpm, but with a lower efficiency due to the loss on the generator acting as a motor.

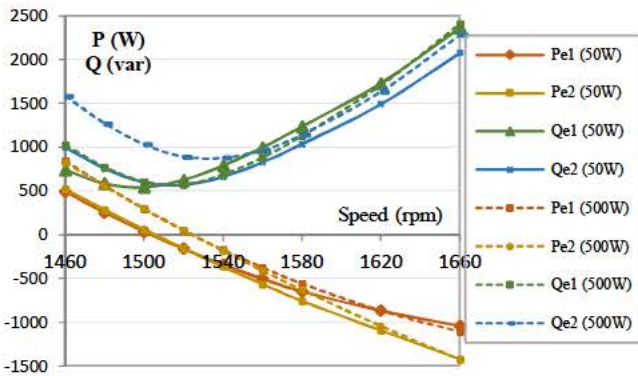


Fig. 9. Real/reactive powers absorbed by excitation winding (P_e , Q_e) vs. rotation speed (rpm). (50W and 500W loads)

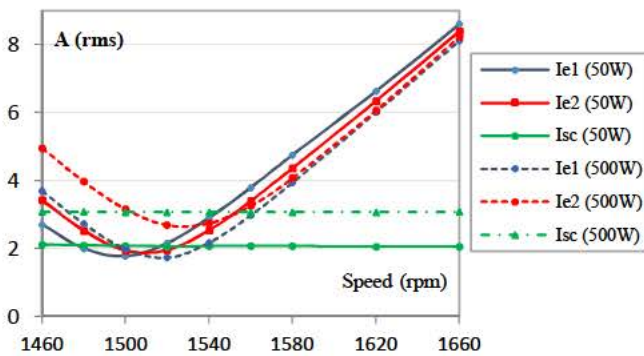


Fig. 10. Stator winding currents vs. rotation speed (rpm). (50W and 500W loads)

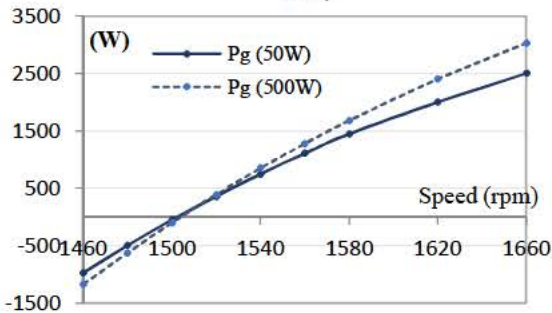


Fig. 11. Total active power generated by the generator (P_g) vs. rotation speed (rpm). (50W and 500W loads)

c) The effect of inputs phase difference

In a three-phase induction generator, optimal performance can be obtained at balanced condition. Since only two of its phases are energized by sinusoidal voltage sources in the proposed OIATI configuration, the generator doesn't necessarily operate at balanced condition. In this study, the excitation capacitor for the output phase is $C=30\mu\text{F}$. The output

voltage is kept at 220Vrms supplying a 500W resistive load ($R_L=96.8\Omega$). The generator is running by a constant-power mechanical load.

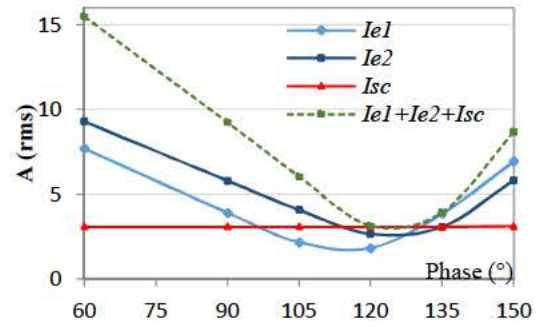


Fig. 12. Phase currents vs. phase difference of V_{e1} and V_{e2} . (630W mechanical input, 500W load)

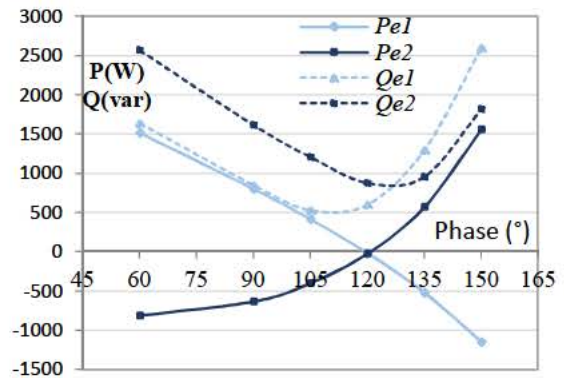


Fig. 13. Power vs. phase difference of V_{e1} and V_{e2} . (630W mechanical input, 500W load)

The optimal angle which minimizes the sum of all winding currents is around 120° based on Fig. 12. This also corresponds to minimal torque ripple as shown in Fig. 14. Similar observation can be found if the generator is running at constant rotation speed. Increasing the phase difference increases real power supplied to the second winding and reduces that of the first winding as depicted in Fig. 13.

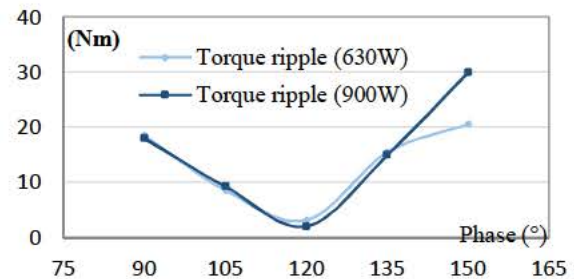


Fig. 14. Torque ripple vs. phase difference of V_{e1} and V_{e2} . (630W and 900W mechanical inputs)

B. Experimental tests

For a validation purposes, experimental results will be compared to simulation results in the following sections. Due to

the limitation of the motor driver, the generator will be rotated at a constant rotation speed and the normal output voltage is limited to 100Vrms at 50Hz. The results recorded during the tests are compared with the results generated in simulation under the same conditions. Experimental and simulated steady-state results of input currents and input active and reactive powers are shown in Fig. 15, Fig. 16 and Fig. 17. For each rotation speed, the excitation input voltages are tuned until a steady-state desired output voltage is obtained. The output terminal is connected to a 30 μ F capacitor and a 29 Ω resistor for an output power of 350W. The test results show that the induction generator follows closely the simulations in terms of active power consumption at the inputs and mechanical power.

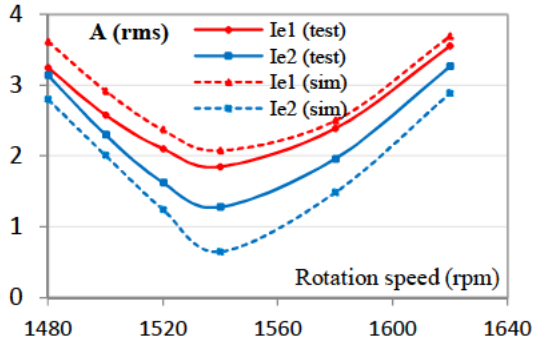


Fig. 15. Test and simulated steady-state results of input currents at different rotation speed.

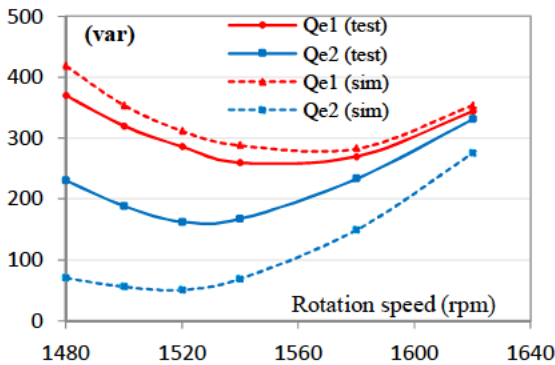


Fig. 16. Test and simulated steady-state results of input reactive powers at different rotation speed.

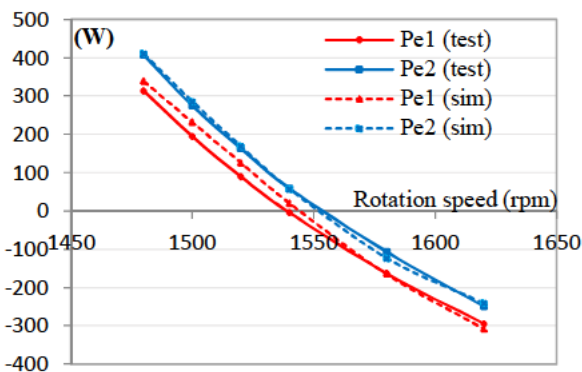


Fig. 17. Test and simulated steady-state results of input active powers at different rotation speed.

Significant differences exist when comparing the results in Fig. 15 and Fig. 16. This may be caused by imperfections of the simulation model which does not include iron losses and saturation. In the model, the prime mover is modelled by constant rotation speed block which is not the accurate model for the generator's shaft driven by another IM. The experimental efficiency of the generator at different speeds is shown in Fig. 18. This efficiency is calculated using different formulas at different operation ranges. At lower speed, the generator acts as motor by the absorbing the active power from inputs. In this case, the input power includes only the input power provided by the excitation terminals. In the middle, the generator and the excitation sources provide the input power. Above a certain speed, the generator provides all the input powers and the output will be also absorbed by the excitation sources. It can be observed that its efficiency drops rapidly below the synchronous speed (1500rpm).

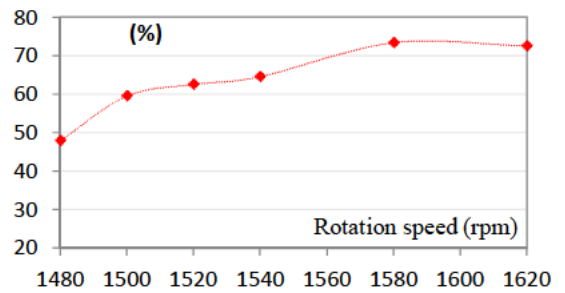


Fig. 18. Generator experimental efficiency at different rotation speeds.

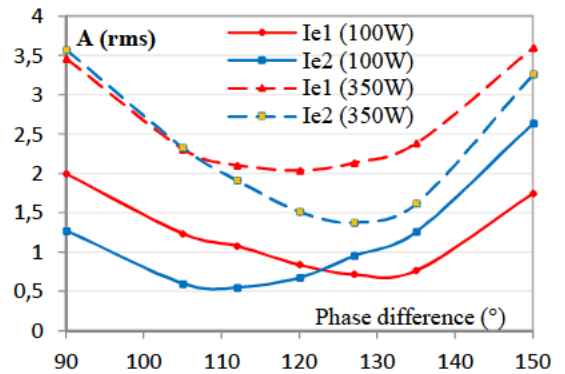


Fig. 19. Steady-state test results of input currents at different phase difference of input voltage sources for 100W and 350W load (at 1520rpm).

The effect of the excitation phase difference is shown in Fig. 19 and Fig. 20 for 100W and 350W loads. In this test, the induction generator's shaft is turned at a fixed rotation speed of 1520rpm. The output voltage is kept at 100Vrms. The output terminal is connected to a 30 μ F capacitor. The rms voltage of both input sources is equal while their phase difference is varied from 90° to 150° ($Ve1$ leads $Ve2$). The comparison of experimental and simulated steady-state values are illustrated in Fig. 21 and Fig. 22.

It can be observed that the optimal angle is once again confirmed at between 120° and 130° angles. For input currents, the optimal angle is slightly increased to about 130° at 350W load from around 120° angles at 100W load.

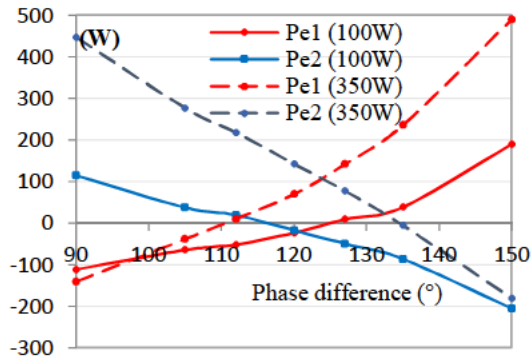


Fig. 20. Steady-state test results of input active powers at different phase difference of input voltage sources for 100W and 350W load (at 1520rpm).

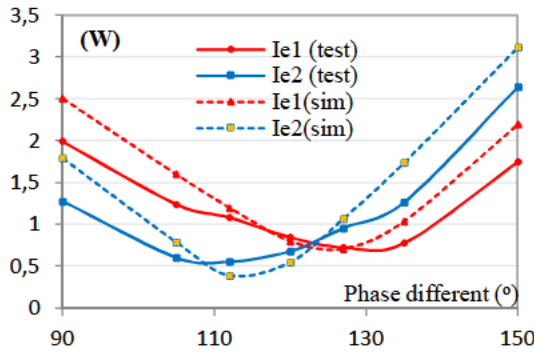


Fig. 21. Test and simulated steady-state results of input currents at different phase difference for 100W load.

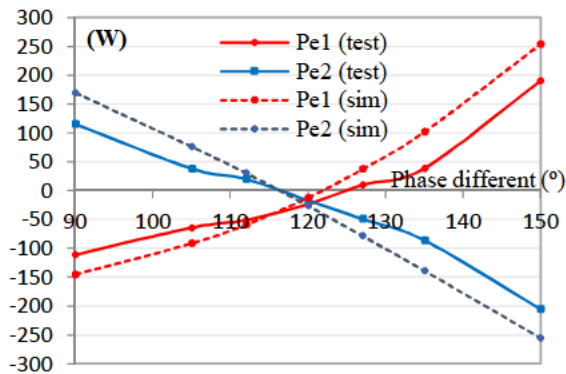


Fig. 22. Test and simulated steady-state results of input active powers at different phase difference for 100W load.

IV. CONCLUSIONS

The study of a newly proposed inverter-assisted configuration, OIATI, for a single-phase generator based on a three-phase induction machine has been described using mathematic model, simulation and experimental tests. Its

dynamic behavior has been modeled and verified with actual tests. Detailed open-loop steady-state behavior of the generator has been carried out using both computer simulation and experimental tests.

Results indicate that the technique allows the generation of electricity at constant frequency while operated at variable speed. However, it is recommended to operate at the range above the synchronous speed to improve the system efficiency. The problem with this is that above the synchronous speed, the generated power is mostly transferred to the excitation inputs and no power is transferred from the excitation inputs to the output. On the other hand, in order to cope with the unbalanced conditions of the machine and to minimize the winding currents, the phase difference of both excitation sources should be around 120° to 130° . Further study might be needed to investigate the control technique of the excitation inputs to achieve balanced operation and optimize the global efficiency of the system.

References

- [1] T.F. Chan, "Performance analysis of a three-phase induction generator connected to a singlephase power system", *IEEE Trans. On Energy Conversion*, vol. 13, pp. 205-213, Sep. 1998.
- [2] T. Fukami, M. Imamura, Y. Kaburaki, T. Miyamoto, "A New Self-Regulated Self-Excited Single-phase Induction Generator Using a Squirrel Cage Three-phase Induction Machine", *Proc. Of the IEEE*, vol. 1, pp. 308-312, Nov. 1995.
- [3] O.J.M. Smith, "Three-phase induction generator for single-phase line." *IEEE Transactions on Energy Conversion*, 1987; PER-7:382-7.
- [4] B. Singh, S.S. Murthy, S. Gupta; "Analysis and design of electronic load controller for self-excited induction generators." *IEEE Transactions on Energy Conversion* 2006; 21:285-93.
- [5] CP. Ion, I. Serban, C. Marinescu; "Single-phase operation of an autonomous three-phase induction generator using a VSI-DL control system." *In: Proceedings of the 11th international conference on optimization of electrical and electronic equipment*; 2008. p. 333-8.
- [6] RQ. Machado, S. Buso, JA. Pomilio, FP. Marafao; "Three-phase to single-phase direct connection rural cogeneration systems." *In: Proceedings of the nine-teenth annual IEEE applied power electronics conference and exposition*; 2004. p. 1547-53.
- [7] EG. Marra, JA. Pomilio; "Self-excited induction generator controlled by a VS- PWM converter providing high power-factor current to a single-phase grid." *In proceedings of the 24th annual conference of the IEEE industrial electronics society*; 1998. p. 703-8.
- [8] UK. Madawala, T. Geyer, JB. Bradshaw, DM. Vilathgamuwa; "A model for a novel variable speed cage induction generator." *In: Proceedings of the 35th annual conference of IEEE industrial electronics*; 2009. p. 59-64.
- [9] U. K. Madawala, D. Muthumani, "A novel variable speed cage induction generator", *Conf. Rec. IEEE ICSET on Sustainable Energy Technologies*, pp. 1250-1255, 2008.
- [10] B. Kim, M. Pietrzak-David, P. Maussion, L. Bun; "Novel Structure of Single-phase Generator from Three-phase Induction Machine: Modeling and Simulation", *IEEE, IECON 2017*, October, Beijing, China.